A *Streptomyces venezuelae* Cell-Free Toolkit for Synthetic Biology

Simon J Moore[1,2,3*], Hung-En Lai[1,2], Soo-Mei Chee[2,5], Ming Toh[1,2], Seth Coode[3], Kameshwari Chengan[3], Patrick Capel[4], Christophe Corre[4], Emmanuel LC de los Santos[4], Paul S Freemont[1,2,5,6*]

[1]Centre for Synthetic Biology and Innovation, Imperial College London, South Kensington Campus, Exhibition Road, London, SW7 2AZ, UK
[2]Department Section of Structural and Synthetic Biology, Department of Infectious Disease; Imperial College London, South Kensington Campus, Exhibition Road, London, SW7 2AZ, UK
[3]School of Biosciences, University of Kent, Canterbury, Kent CT2 7NJ, UK
[4]Warwick Integrative Synthetic Biology Centre, School of Life Sciences, University of Warwick, Gibbet Hill Road, Coventry, CV4 7AL, UK
[5]The London Biofoundry, Imperial College Translation & Innovation Hub, White City Campus, 80 Wood Lane, London W12 0BZ, UK
[6]UK Dementia Research Institute Care Research and Technology Centre, Imperial College London, Hammersmith Campus, Du Cane Road, London, W12 0N

Keywords
Cell-free synthetic biology, *Streptomyces*, natural products, *in vitro* transcription-translation, cell-free protein synthesis

*Joint corresponding authors: Dr Simon Moore (S.J.R.Moore@kent.ac.uk) and Professor Paul Freemont (p.freemont@imperial.ac.uk)

Abstract
Prokaryotic cell-free coupled transcription-translation (TX-TL) systems are emerging as a powerful tool to examine natural product biosynthetic pathways in a test-tube. The key advantages of this approach are the reduced experimental timescales and controlled reaction conditions. To realise this potential, it is essential to develop specialised cell-free systems in organisms enriched for biosynthetic gene clusters. This requires strong protein production and well-characterised synthetic biology tools. The *Streptomyces* genus is a major source of natural products. To study enzymes and pathways from *Streptomyces*, we originally developed a homologous *Streptomyces* cell-free system to provide a native protein folding environment, a high G+C (%) tRNA pool and an active background metabolism. However, our initial yields were low (36 µg/mL) and showed a high level of batch-to-batch variation. Here, we present an updated high-yield and robust *Streptomyces* TX-TL protocol, reaching up to yields of 266 µg/mL of expressed recombinant protein. To complement this, we rapidly characterise a range of DNA parts with different reporters, express high G+C (%) biosynthetic genes and demonstrate an initial proof of concept for combined transcription, translation, and biosynthesis of *Streptomyces* metabolic pathways in a single ‘one-pot’ reaction.

Introduction

Streptomyces bacteria are environmental specialists (e.g., soil, marine, desert) that synthesize rich repertoires of natural products such as antibiotics. Much of this genetic information is locked up and cryptically regulated within biosynthetic gene clusters; regions of genomic DNA that harbor enzymes and other proteins (e.g., transporters, resistance markers). The key limitation in awakening these clusters for natural product discovery, is silent gene expression and recalcitrant genetics. Traditional strategies to overcome this include genetic modification of the host organism to bypass native regulatory elements, and the 'capture' of the cluster and expression in a heterologous host[1]. But this can take several weeks to months to complete with varying levels of success: some cryptic clusters remain dormant due to obscure native regulation. Fundamental tools that aid these efforts, are of major interest to the natural product community.

Prokaryotic cell-free coupled transcription-translation systems are emerging as a new tool for studying natural product biosynthesis[2–9]. Cell-free transcription-translation uses a crude cell-extract or purified ribosomes and translation factors – the PURE system - in a 'one-pot' reaction[10,11]. *E. coli* cell-extracts, referred to as either TX-TL[5,12,13] or cell-free protein synthesis (CFPS)[4,14], are low-cost, straightforward to prepare and provide high recombinant protein yields, of up to 2300 µg/mL[15]. Moreover, metabolism is active[16], providing ATP regeneration, while amino acid pathways are dynamic, providing additional ATP (through L-glutamate). In addition, certain amino acids deplete and become limiting for protein synthesis[17]. In summary, TX-TL provides distinct opportunities for natural product biosynthesis: precursors for biosynthesis, direct control to feed precursors, short experimental timescales (4-24 hours), and stable yields. Moreover, we and others have shown the potential for automation in cell-free[18–23]. Specifically, we have screened up to 500 plasmid variants in 24 hours[23].

While *E. coli* TX-TL and the PURE system are promising for natural product biosynthesis[2–4,9], *E. coli* has limited potential for studying biosynthetic gene clusters from *Streptomyces*, due to a number of genetic and metabolic differences. For example, the codon content between *Streptomyces* (~70% G+C) and *E. coli* (51% G+C) is different, while the regulatory sequences that control transcription, post-transcription and overall gene expression are distinct. Moreover, secondary metabolism in *E. coli* is not necessarily well-suited, and often requires further metabolic engineering. Notwithstanding, *E. coli* synthesis of heterologous proteins can result in poor expression and solubility[5,24]. Therefore, we anticipate that a dedicated *Streptomyces* TX-TL system for homologous protein synthesis, has several advantages for studying natural product biosynthesis. As a first step, we originally released a *Streptomyces venezuelae* DSM-40230 (ATCC 10712) TX-TL system, but this produced low protein yields (36 µg/mL) with high batch-to-batch variability. We chose *S. venezuelae* ATCC 10712 since it is well-suited to synthetic biology. *S. venezuelae* ATCC 10712 is fast-growing (40 min doubling time) and grows dispersedly in liquid culture; most *Streptomyces spp.* have slower doubling times and clump in mycelial aggregates. Moreover, *S. venezuelae* has a range of synthetic biology tools[25,26] and is an attractive host for industrial biotechnology[27,28]. In parallel to our studies, the Jewett group[7] also established a *Streptomyces lividans* CFPS system (yields ~50 µg/mL), which was further optimised[29]. A recent update to this system highlighted the need for adding individual purified translation factors[8] to elevate protein synthesis up to ~400 µg/mL.

Based on this, we rationalized that protein synthesis, in our original *S. venezuelae* TX-TL system, could be limited by the use of an energy solution derived for an optimal *E. coli* TX-TL protocol[12]. For a review of the biochemical role and origin of cell-free energy solutions, we refer the reader to Dopp *et al*[30]. In brief, TX-TL requires a cell-extract, a primary and secondary energy source, amino acids, cofactors, molecular crowding agents, additives (e.g., Mg^{2+}, spermidine, folinic acid, tRNA) to support protein synthesis from a template DNA sequence. Some of these biochemicals are present in the cell-extract but may be rate-limiting. The energy source is composed of nucleotide triphosphates to drive initial mRNA and protein synthesis (primary energy source) and commonly 3-phosphoglyceric acid (3-PGA) or phosphoenolpyruvate (PEP) as the secondary energy source. 3-PGA or PEP provide ATP regeneration to leverage extended protein synthesis. Potentially, primary metabolism could be activated in TX-TL to provide reducing equivalents (e.g. NADH, FADH), extra energy and building blocks (e.g. amino acids, malonyl-CoA) for natural product biosynthetic pathways, as shown in cell-extract metabolic engineering[31]. In this work, we focus on upgrading our *S. venezuelae* system to elevate protein synthesis. We also demonstrate its broader potential for cell-free synthetic biology, namely for characterising DNA parts and activating some model biosynthetic pathways. To achieve this, we made some simple modifications to the system, allowing yields of up to 266 µg/mL of expressed recombinant proteins. We also demonstrate combined transcription-translation and biosynthesis of some example natural product pathways, namely melanin and haem biosynthesis. We report an easy-to-follow protocol that simply requires three components: DNA, cell-extract and a master mix that we describe in detail. We believe this generic *Streptomyces* TX-TL toolkit will be of broad interest to the natural product community, complementing experimental wet-lab tools for genome mining studies.

Results and discussion

A high-yield *Streptomyces* TX-TL protocol

To provide an improved *Streptomyces* TX-TL toolkit for synthesis of high G+C (%) genes and pathways from *Streptomyces* spp. and related genomes, a key priority was to optimise protein production. Also, a straightforward protocol with minimal batch variation was essential, for ease of repeatability. Since bacterial transcription and translation is coupled, either these steps, physical parameters or components from the energy solution, limit overall TX-TL activity. Therefore, to keep our protocol streamlined, we made the following changes: promoter strength, energy solution, ATP regeneration and RNAse inhibition. In doing so, we obtained a high-yield protocol with minimal variation between different cell-extract batches (Figure 1A).

Promoter strength – Previously, we used the *kasOp** promoter to drive mRNA synthesis in *Streptomyces* TX-TL. This yielded up to 1.3 µM (36 µg/mL) of the model superfolder green fluorescence protein (sfGFP) in our previous work[5]. Promoter strength is a key limiting factor in heterologous expression systems. *kasOp** is a strong *Streptomyces* constitutive promoter, originally derived from the *kasO*/*cpkO*/*sco6280* promoter, with core -35 and -10 boxes of TTGACN and TAGART, respectively[32]. The *kasOp** promoter is active in a range of *Streptomyces* spp. through the endogenous RNA polymerases and HrdB house-keeping Sigma factor[32]. Bai *et al* developed a synthetic promoter library based around *kasOp**, using fluorescence-activated cell sorting (FACS) to quantity *S. venezuelae* protoplasts[25]. This included the isolation of a synthetic promoter 44 (SP44), which is 1.87-fold stronger than *kasOp**[25]. We used *Streptomyces* TX-TL to test a panel of promoters developed by Bai *et al*, with SP44 being the strongest (2.63 µM sfGFP) and 2.2-fold more active than *kasOp** (Figure 1B). We also repeated this across four independent cell-extract batches, but still observed strong batch variation. However, SP44 provided a stronger reporter plasmid to continue the optimisation process.

Energy solution – Next, we focused on developing a minimal energy solution (MES) to identify any non-essential components. The standard *E. coli* TX-TL energy solution used previously[5], is composed of HEPES buffer, ions (e.g. Mg-glutamate, K-glutamate), nucleotide triphosphates (NTPs - ATP, GTP, CTP and UTP), secondary energy source [typically 3-phosphoglyceric acid (3-PGA) or phosphoenolpyruvate (PEP)], amino acids, molecular crowding agent and a number of additives[14]. To establish a MES for *Streptomyces* TX-TL, we first eliminated a number of non-essential components from the energy solution. This included coenzyme A, tRNA (*E. coli*), NAD, cAMP, folinic acid and spermidine (Figure S1A). While we did initially observe a positive response with cAMP, after several repeats in batches, this effect was not repeatable. For the HEPES buffer component, this was non-inhibitory (10-100 mM) and provided optimum activity between pH 8-9 (Figure S1B). For the secondary energy source, we found 3-PGA was essential; the removal of 3-PGA decreased sfGFP synthesis by 98% (Figure S1C). We tried to replace 3-PGA with alternative secondary energy sources but observed only minimal activity: maltose (0.13 µM), sucrose (0.15 µM) and pyruvate (0.17 µM). Other potential sources such as glucose (with phosphate), PEP and succinate were inactive (Figure S1C). 3-PGA is the preferred secondary energy source in a range of non-model cell-extract hosts[33], due to its chemical stability and high energy potential, with an optimum concentration of 30 mM (Figure S1D). For the primary energy source (NTPs), there was some basal

activity without additional NTPs but addition of 3 mM ATP/GTP and 1.5 mM CTP/UTP provided peak activity (Figure S1E). Surprisingly, the removal of amino acids only decreased sfGFP synthesis by 45%, with 0.5-1.5 mM amino acids providing peak activity (data not shown). For a Mg screen, we found that $MgCl_2$, Mg-glutamate or Mg-acetate were all active (Figure S1F), while high levels of K-glutamate (150-200 mM) stimulated increased sfGFP synthesis (Figure S1F). This is possibly due to additional ATP regeneration via entry of α-ketoglutarate into the TCA cycle, as previously shown [34]. Lastly, while we observed reasonable activity without PEG, 1% (w/v) PEG 6K was optimum, providing a 44% rise in activity (Figure S1G). However, it is desirable to omit PEG for downstream natural product analytical purposes (e.g., LC-MS). Finally, based on these observations, we optimised our basic *Streptomyces* TX-TL MES system by individually fine-tuning the concentration of its core components (3-PGA, NTPs), while leaving DNA (40 nM), Mg-glutamate (4 mM), K-glutamate (150 mM), amino acids (1.25 mM) and PEG 6K (1%) constant. 3-PGA was most optimum at 30 mM, while the NTP level (ratio of 2:1 ATP/GTP:CTP/UTP), showed biphasic activity, peaking at 3 mM ATP/GTP, with full inhibition at 4 mM. Specific data on Mg-glutamate and K-glutamate optimisation with four different cell-extract batches is presented in Figure S2. As a combined result of this optimisation process, sfGFP synthesis was increased to 4 μM, representing a 52% increase.

Additional ATP regeneration pathways - In a previous study, Caschera *et al* highlighted that other glycolytic enzymes function in *E. coli* TX-TL, using the disaccharide maltose (or maltodextrin) combined with 3-PGA. This method extended protein synthesis up to 10 hours, through inorganic phosphate recycling[15]. We investigated whether this part of metabolism is functional in *Streptomyces* TX-TL. Therefore, we tested the *Streptomyces* MES system (with 3-PGA) with maltose, glucose, glucose-6-phosphate (G6P) or fructose-1,6-phosphate (F16P). Interestingly, maltose, glucose, Glc6P, and F16P all prolonged the length of *Streptomyces* TX-TL activity from 2 to 3 hours. This was maximal with 5 mM Glc6P and 30 mM 3-PGA (Figure 1C), at an optimum temperature of between 24-28°C (Figure 1D). All together we observed a 59% increase in sfGFP synthesis to 6.37 μM, but lower levels of NTP are required (Figure 1C) – equivalent to 1 mM ATP/GTP and 0.5 mM CTP/UTP. We speculate this could be related to ATP regulation of the glycolytic enzymes (e.g., hexokinase, fructokinase), leading to rapid depletion of ATP and inhibition of protein synthesis. However, this requires further investigation as there is limited literature on specific glycolytic enzymes from *Streptomyces*.

RNAse inhibition – As a final addition to the system, we tested the effect of the inexpensive RNAse inhibitor, polyvinylsulphonic acid (PVSA). Recently, PVSA, an RNA-mimetic, was shown to improve mRNA stability in *E. coli* TX-TL, but did not increase protein synthesis[35]. In *Streptomyces* TX-TL, 1 mg/mL PVSA increased sfGFP synthesis up to 5.87 μM, in the basic MES system (Figure 1E). However, while we observed individual improvements with either the PVSA RNase inhibitor or the blended G6P/3-PGA secondary energy source, in combination, there was no significant additive effect with PVSA and G6P/3-PGA together. This suggested that other rate-limiting factors are at play.

In summary, we have made a specific energy solution for *Streptomyces* TX-TL with an overall six-fold improvement in the system. This is attributed to the combined use of 3PGA and G6P as secondary energy sources and a stronger promoter system.

Furthermore, we find this can be combined into a single *Streptomyces* master mix (SMM) solution, further streamlining the reaction process. With this simple modification, the TX-TL reaction requires three single components that minimises batch variation: SMM solution, plasmid DNA and the cell-extract. Next, we sought to demonstrate the use of this simplified system for the testing of plasmid tools and regulatory elements for *Streptomyces* synthetic biology.

Cell-free characterisation of *Streptomyces* genetic tools for synthetic biology

It is highly desirable to characterise standard DNA parts using rapid and iterative design-build-test-learn cycles - the central paradigm of synthetic biology. For *Streptomyces* and related strains, either conjugation or protoplast transformation is typically used to transfer self-replicating and integrative plasmids for the testing of DNA parts for *Streptomyces* synthetic biology[25,26,32]. DNA parts are small modular regulatory elements (e.g., promoter, insulator, tags, RBS, ORF, terminator) that facilitate downstream combinatorial DNA assembly workflows (e.g., Golden Gate) for refactoring gene expression pathways. While there are different approaches to quantitate gene expression[26,36], Bai *et al*[25] recently applied a lysozyme method, to study single-cell gene expression quantitation of *S. venezuelae* ATCC 10712 protoplasts using fluorescence-activated cell sorting.

We next tested the promoter and RBS elements from Bai *et al*[25] in *Streptomyces* TX-TL, as well as two other important regulatory elements: alternative start codons[36] and terminators[37]. Firstly, we built these DNA parts to be compatible with our previous DNA assembly method, EcoFlex[38]. For this we had to modify the promoter consensus (prefix renamed, e.g., SP44a instead of SP44) to remove an internal BsmBI site to permit MoClo assembly. In addition, to provide comparative *in vivo* data, we built a new destination vector (cured of BsmBI and BsaI sites) from pAV-*gapdh* from Phelan *et al*[26] and renamed this StrepFlex (pSF1). pAV-*gapdh* is an integrative shuttle vector developed as a synthetic biology plasmid tool for *S. venezuelae*[26]. Firstly, for the promoter library (*kasOp**, SP15a, SP19a, SP23a, SP25a, SP30a, SP40a, SP44a and *ermEp**), we assembled this with the RiboJ insulator, R15 capsid RBS, mScarlet-I and the Bba_B0015 terminator. For the RBS library, *kasOp** was used as the promoter. For the promoter variants, activity ranged from 5% (*ermEp**) to 100% (*kasOp**). In contrast to earlier results (Figure 1B), the range of activities for the BsmBI cured promoter variants were between 30-50% less active across the library. For the activity of the RBS variants, this ranged from 0.7% (SR9) to 117% (SR39) activity relative to the R15 capsid RBS (Figure 2B). We also tested two-dimensional promoter and RBS space with sfGFP (Figure 2C). Lastly, to provide *in vivo* data, we characterised the mScarlet-I promoter and RBS plasmids (from Figure 2A and 2B) in *S. venezuelae* ATCC 10712 (Figure S3) following the approach by Phelan *et al*[26]. Interestingly, there was some significant outliers in the RBS library. SR39 (along with the *E. coli* PET-RBS) was the strongest RBS in contrast to SR40, which was unexpectedly weaker both *in vitro* and *in vivo*. In addition, SR4, an expected weak RBS, was strong in both *in vitro* and *in vivo* measurements (Figure 2A-2B, Figure S3). This may reflect differences in the upstream 5'-untranslated (5'-UTR) region and the use of a different fluorescence reporter (mScarlet-I), in comparison to Bai *et al*[25]. However, overall the promoter and RBS strengths characterised were broadly consistent with the original publication[25].

Another important regulator of gene expression is the start codon. In most bacteria, ATG is the preferred codon for translation initiation through fMet-tRNA. Previously, Myronovskyi *et al* used a β-glucuronidase (GUS) reporter to show that the TTG codon was stronger than ATG for translation initiation by almost 2-fold in both *Streptomyces albus* J1074 and *Streptomyces sp.* Tu6071[36]. Using sfGFP and mScarlet-I as reporters, our findings suggest that, for *S. venezuelae* at least, ATG is equivalent in strength to TTG, followed by CTG and lastly GTG as the weakest (Figure 2C). This also likely changes with coding sequences and 5'-UTR. In comparison, for *E. coli* the order of strength goes as follows: ATG > GTG > TTG > CTG[39]. We expect this differs due to high GC codon bias in *Streptomyces*. Despite the use of different experimental conditions, our results confirm that TTG is a strong alternative start codon and that GTG is weak. Nevertheless, the role of GTG in regulation is unclear and intriguing due its high frequency in *Streptomyces* genomes[40].

To the best of our knowledge, no studies have so far reported the use of terminators for controlling pathway expression in *Streptomyces*. Using the same experimental format as we previously used in EcoFlex[38], we tested a selection of Rho-independent terminators from the iGEM catalogue (Bba_B0012, Bba_B0015) and from Chen *et al*[41] in *S. venezuelae* TX-TL (Figure 2D). The latter terminators were designed to prevent repetition in DNA elements and protect against homologous recombination as previously highlighted[41,42]. In summary, the activities we observed, strongly follow our previous observations in *E. coli* cell-free[38]. For now, our TX-TL system demonstrates proof-of-concept data for prototyping DNA parts in *Streptomyces*. Rho-independent terminators may in future provide tools for refactoring metabolic pathways in engineered *Streptomyces* strains.

TX-TL synthesis of high G+C (%) genes

Previously, we found our *Streptomyces* TX-TL system was most active with 40 nM of plasmid DNA, using the *kasOp**-sfGFP reporter, to saturate protein synthesis[35]. In comparison to *E. coli* TX-TL, protein synthesis is saturated at around 5-10 nM of reporter DNA, which varies with different promoters and sigma factors[43]. We questioned whether DNA degradation led to this discrepancy since most *Streptomyces spp.* degrade methylated plasmid DNA with endonucleases[44]. To compare methylated and unmethylated plasmid DNA for methylation-specific endonucleases, we tested unmethylated and methylated SP44-sfGFP reporter plasmid in *Streptomyces* TX-TL. Interestingly, there was no major change in sfGFP synthesis between unmethylated and methylated plasmid DNA, across different DNA concentrations (Figure S4). We also tested relative plasmid DNA stability in *S. venezuelae* cell-extracts, with the standard MES energy solution, and incubated at different time-lengths, followed by re-extraction of the plasmid DNA (using the Qiagen plasmid DNA purification kit). The extracted plasmid DNA was then separated and visualised on a 1% (w/v) agarose gel. This indicated that methylated plasmid DNA is stable, during the time (0-4 h) when TX-TL is active (Figure S4). Further to this, we tested linear DNA for exonuclease activity. To protect the coding sequences, we PCR amplified about 150-250 bases upstream and downstream of the coding parts, using the standard SP44-sfGFP reporter plasmid. However, in the TX-TL reaction, linear DNA was 95% less active than circular DNA, at 40 nM of DNA (Figure S5). This suggests the *S. venezuelae* cell-extract has exonuclease activity, while endonuclease activity is minimal.

Since circular DNA degradation was not a limiting factor, we tested different fluorescent proteins (Figure 3A) to determine if the optimum plasmid DNA concentration for protein synthesis changes. Firstly, we tested mVenus-I and mScarlet-I, combined with the strong SP44 promoter, and compared them to the SP44-sfGFP reporter. The maximum yields achieved for these three proteins were: 6.48 µM sfGFP (174 µg/mL), 9.50 µM mScarlet-I (266 µg/mL) and 7.72 µM mVenus-I (224 µg/mL). Interestingly, this was tested in the extract batches presented in Figure S2, where both SP44-mScarlet-I and SP44-mVenus saturated protein synthesis with a lower DNA template (10 nM) than SP44-sfGFP (50 nM) (Figure 3B). This was surprising since the coding sequence of mVenus is 96% identical to sfGFP, with the exception of 30 mutations and an additional GTG (valine) at the second codon for mVenus-I. However, while the optimal sfGFP plasmid DNA concentration was 50 nM in this experiment, consistent with our previous work[5], it was not consistent in all extract batches (Figure S4B). This contrasting result likely relates to either a difference in mRNA stability or translation initiation rate between the batches. Since little is known about how *Streptomyces sp*. control protein synthesis, this topic alone merits a separate in-depth investigation.

Secondly, we tested the robustness of the system for other proteins from high G+C (%) genes (Figure 3C).We expressed the oxytetracycline enzymes (OxyA, -B, -C, -D, -J, -K, -N and -T) from *Streptomyces rimosus* that were previously only detectable by Western blotting in our original publication[5], as well as three non-ribosomal peptide synthetases (NRPS). The latter included the TxtA and TxtB NRPS enzymes from thaxtomin A biosynthesis in *Streptomyces scabiei* and an uncharacterised NRPS (NH08_RS0107360) from *S. rimosus*. Except for TxtA, most enzymes were discernible by either SDS-PAGE (Figure 3C), while for OxyA (47 kDa) and TxtB (162 kDa), low levels (<0.5 µM) were detected by Western blotting using an anti-Flag tag (data not shown). We also incorporated a C-terminal tetracysteine tag with the oxytetracycline enzymes and mScarlet-I, using the fluorogenic biarsenical dye fluorescein arsenical hairpin binder-ethanedithiol (FlAsH-EDT_2), to measure real-time nascent protein synthesis (Figure 3D). Most oxytetracycline enzymes showed a significant increase in FlAsH-EDT_2 fluorescence ($P < 0.05$), peaking at 120 min, with only OxyN producing the weakest response ($P = 0.056$). However, this was still clearly detectable by PAGE or Western. For mScarlet-I, the time-lag between the fluorescence signals for FlAsH-EDT2 (immature protein) and mScarlet-I (mature protein) allowed us to estimate a maturation time of 40 min for mScarlet-I (Figure 3E). This is in close agreement to a literature value of 36 min, calculated *in vivo*[45]. In summary, our *Streptomyces* TX-TL system is robust for expression of high G+C (%) genes, incorporates multiple tools (e.g., tags, plasmid systems) and is comparable to other bacterial TX-TL systems.

Transcription, translation and biosynthesis

The next step was to reconstitute a biosynthetic pathway in *Streptomyces* TX-TL system. Initially, to show the synthesis of a single enzyme and its activity, we selected the GUS reporter enzyme. We synthesised the enzyme in the TX-TL reaction from 40 nM SP44-*gus*, left for 4 h at 30°C. The GUS enzyme showed a clear band on SDS-PAGE at the expected size of 68 kDa (Figure S6). To test for GUS activity, an equal volume of the TX-TL extract, as well as a negative control reaction, was mixed with X-GlcA substrate in increasing concentrations (10, 25 and 50 mg/mL). Only the extract from the SP44-*gus* reaction developed a deep blue pigment within minutes, indicating strong GUS activity (Figure 4A).

Next, we selected two metabolic pathways to provide a further test for the TX-TL system. We selected two operons from *S. venezuelae* encoding the melanin and early-stage haem biosynthetic pathways to provide a discernible output for testing (fluorescence and/or colorimetric). Also, both operons were selected from *S. venezuelae*, to improve expression in TX-TL since the codon usage is adapted to this host.

Melanin is a natural pigment that absorbs ultraviolet (UV) light to protect cells from DNA damage. Recently, Matoba *et al* studied the mechanism of tyrosinase and the role of the "caddie" protein from *Streptomyces castaneoglobisporus* HUT6202[46]. Tyrosinase, TyrC, catalyses the rate-limiting step in melanin biosynthesis. It oxidises the phenol group (in L-tyrosine) into the *orthro*-quinone intermediate, which enters an autocatalytic cascade into the melanin pathway. TyrC is dicopper-dependent, with each Cu(II) atom coordinated by three His residues, facilitated by MelC1, a small (12.8 kDa) metallochaperone. The *S. venezuelae* tyrosinase operon encodes both MelC1 and TyrC. After TX-TL with SP44-*melC1-tyrC*, denaturing PAGE shows clear synthesis of TyrC at approximately 34 kDa (expected 31.4 kDa) although MelC1 was indistinguishable (Figure S7). In terms of activity, we observed brown pigment formation after ~2 hours, only with the addition of 1 mM $CuCl_2$ (Figure 4B). This indicates L-DOPA formation, which enters an autocatalytic cascade, leading to different melanin pigments. This suggests TyrC is active, despite the apparent absence of MelC1. Without the addition of $CuCl_2$ or tyrosinase plasmid, the cell-extracts remained clear. Previously, Matoba *et al* showed that insertion of Cu(II) into TyrC by MelC1 involves a transient interaction, and that MelC1 is unstable and forms aggregates difficult to detect with PAGE[46]. Also, apo-TyrC is inactive with Cu(II) alone, which suggests that our TX-TL system supports the synthesis of both TyrC and MelC1.

Lastly, we tested a three-gene biosynthetic operon (*hemC-hemD*/*cysG*^{A}-*hemB*) that catalyses the early-stages of haem biosynthesis[47]. This pathway was selected since it contains a known fluorescence reporter enzyme CysG^{A} [48], a methyltransferase naturally fused as HemD/CysG^{A}. We added a pTU1-A-SP44-*hemC-hemD*/*cysG*^{A}-*hemB* (pTU1-A-SP44-*hem*) plasmid into the TX-TL reaction, as well as a negative control plasmid (pTU1-A), both with and without 5-aminolevulinic acid (5-ALA), which is the substrate for the pathway. In the presence of pTU1-A and 1 mM ALA, there was some minor background fluorescence (Figure 4C), which we expected since haem biosynthesis is essential. In contrast, with pTU1-A-SP44-*hem* and 1 mM ALA, strong red fluorescence was generated, 20-fold higher than background levels in the control reaction (pTU1-A and 1 mM ALA). For protein synthesis, while we could detect HemB (35 kDa) and HemC (38 kDa), the fusion protein HemD/CysG^{A} was less clear, with other major bands at the expected mass – 58.3 kDa (Figure S6). To verify pathway function, we ran a semi-continuous reaction[7] to facilitate purification by separating the haem intermediates from the cell-extract proteins (inset image in Figure 4C). Interestingly, LC-MS analysis detected the air-oxidised product of the HemD enzyme (uroporphyrinogen III - 837 m/z), observed as a 6-electron oxidised uroporphyrin III (red fluorescent) intermediate at 831 *m/z*, typical for these air-sensitive intermediates (Figure S8-S9). Since uroporphyrinogen III is colourless and non-fluorescent, we tried to minimise oxygen levels in the TX-TL reaction using a layer of mineral oil in small-scale batch reactions. Surprisingly, the pigment and fluorescence still accumulated, suggesting that dissolved oxygen levels remain stable in the cell-extract. Interestingly,

we also found the TX-TL reactions were still active for sfGFP and mScarlet-I synthesis (data not shown). This anaerobic activity potentially suggests that oxygen is not rate-limiting at the current level of protein synthesis activity and is sufficient for folding of the fluorescence proteins. Further investigation is needed to determine whether oxidative phosphorylation is active in *Streptomyces* TX-TL and whether this presents a bottleneck to overall ATP regeneration. In summary, these results show that our *S. venezuelae* TX-TL system can support the synthesis of at least three enzymes from plasmid DNA in a combined 'one-pot' translation, translation and enzymatic pathway.

Conclusions

Our study complements a recent surge in interest in the use of cell-free systems for the study of biosynthetic pathways[2,4,9,29]. Here we wanted to expand the palette of plasmid tools for the further development of *S. venezuelae* as a synthetic biology chassis by developing an optimised streptomyces TX-TL toolkit[5,25–27]. Our combined findings show at least a six-fold improvement in protein synthesis over our original *Streptomyces* TX-TL system, using the wild-type *S. venezuelae* ATCC 10712 strain. It is likely genetic modifications that either limit RNA degradation or increase translation rates will improve this current system. Indeed, Xu *et al* recently showed translation factors are a clear rate-limiting step for other *Streptomyces* cell-free systems[8]. Finally, we demonstrate that the semi-continuous system permits reasonable milligram scale-up of biosynthetic metabolites and a clean route to purification and analysis. In conclusion, our results realise the early-stage potential of *Streptomyces* cell-free for the study of synthetic biology for natural products. It provides a native prototyping environment for developing synthetic biology tools (e.g., promoters/RBS) and also for exploring biosynthetic pathways from these organisms.

Methods

Molecular biology

All plasmids were either prepared using EcoFlex cloning or by routine materials and methods, as previously described[41]. For PCR of high GC genes and operons, Q5 polymerase (NEB, UK) was used, using standard cycling or touchdown (72-59°C annealing) and the addition of 5% (v/v) DMSO. For tricky amplicons, the protocol was modified with an annealing time of 30 seconds and elongation temperature reduced to 68°C. The following bacterial strains were used: *S. venezuelae* DSM-40230 and *E. coli* DH10β. Unmethylated plasmid DNA was prepared from an *E. coli dam*$^-$ *dcm*$^-$ mutant (C2925) obtained from NEB. Plasmids and oligonucleotides are listed in Table S1-S4.

Preparation of cell-extracts

S. venezuelae ATCC 10712 was grown in GYM (prepared in distilled water). The cell-extracts were prepared as described previously[5], with the exception that β-mercaptoethanol was removed from the wash buffers and replaced with 2 mM dithiothreitol.

Energy solution and reaction conditions

The reaction mixture contained: 8 mg/mL cell-extract, 25 mM HEPES, 1 mM ATP, 1 mM GTP, 0.5 mM UTP, 0.5 mM CTP, 30 mM 3-PGA, 5 mM glucose-6-phosphate, 1.5 mM amino acids (1.25 mM L-leucine), 4 mM Mg-glutamate, 150 mM K-glutamate, 1% (w/v) PEG6K and 5 mg/mL PVSA. All reactions were incubated at 28°C, with 40 nM pTU1-A-SP44-sfGFP and the MES or SMM buffer system, unless otherwise stated. At least three technical repeats were prepared (for fluorescence measurements) and repeated with at least two independent cell-extract batches (from A6-A9) prepared on separated days. See Table S6 for chemicals in the SMM buffer.

Denaturing PAGE

40 µL cell-free reaction (30 µL SMM + 10 µL plasmid DNA) was incubated in a 2 mL tube at 25-30°C (no shaking) for 6 hours. To precipitate proteins, 1 mL ice-cold 100% (v/v) acetone was added. Samples were placed at -20°C for 30 mins, before centrifugation at 18,000 × *g*, 4°C for 10 min. The supernatant was removed, and the pellet was washed with 1 mL ice-cold 70% (v/v) acetone. Centrifugation and supernatant removal steps were then repeated. The pellet was air-dried, before re-suspending in 30 µL ddH_2O and 10 µL 4X NuPAGE lithium dodecyl sulphate (LDS) sample buffer (ThermoFisher) and boiled at 100°C for 5 min. To ensure the pellet was solubilized, samples were aspirated with a pipette five times, and if necessary (a visible pellet remaining), left for an additional 5 min at 100°C. 10-100 µg total protein was then separated with a 4-12% (v/v) gradient Bis-Tris gel (ThermoFisher) run in MES buffer system. Proteins were stained with InstantBlue (Generon), destained with ddH_2O and images were recorded with the ChemiDoc XRS imaging system (Biorad).

TX-TL fluorescence measurements

10 µL cell-free reactions were prepared in a 384-well black Clear®, F-bottom, low-binding plate (Greiner). Reactions were measured as a triplicate technical repeat and at least repeated with cell-extracts prepared from two separate days. They were measured in a 384-well plate. The plate was sealed with aluminium film, SILVERseal™ (Greiner), briefly centrifuged at 2,000 × *g* for 10 seconds. Real-time

plate measurements were recorded in a CLARIOStar© plate reader (BMG Labtech, Germany) at 30°C with 10 seconds of shaking at 500 rpm prior to measurements, using either standard filters (Omega) or monochromator settings (CLARIOStar). Purified sfGFP, mVenus-I and mScarlet-I standards were purified, as described previously[5], to estimate protein concentration during real-time fluorescence measurements.

Mass spectrometry analysis

TX-TL reactions were prepared as two components (A and B) in a semi-continuous reaction as follows: Component A - 100 µL of standard TX-TL reaction, in the absence of PEG, was injected into a Thermo Scientific Pierce 3.5K MWCO 96-well microdialysis device; Component B - 1.5 mL SMM solution with 1 mg/mL carbenicillin, in a 2.5 mL tube. The microdialysis cassette was placed inside the 2.5 mL tube and incubated at 30°C for 24 h with shaking (1000 rpm). Samples were acidified with 1% (v/v) HCl, centrifuged at 18,000 x *g* for 25 min at room temperature. The supernatant was loaded onto a Sep-Pak C-18 (50 mg sorbent) solid-phase extraction cartridge (Waters), washed with 10 mL of 10% (v/v) ethanol and eluted with 2 mL of 50% (v/v) ethanol. All solutions were acidified with 1% (v/v) HCl. Eluted samples were dried under vacuum at room temperature, using an Eppendorf Concentrator Plus. Samples were dissolved in 150 µL 1% (v/v) HCl and centrifuged again at 18,000 x *g* for 25 min at room temperature. 1 µL of supernatant was then analysed by LC-MS, performed with an Agilent 1290 Infinity system with an online diode array detector in combination with a Bruker 6500 quadruple time-of-flight (Q-ToF) mass spectrometer. An Agilent Extend-C18 2.1 x 50mm (1.8 µm particle size) column was used at a temperature of 40°C with a buffer flow rate of 0.5 mL/min. LC was performed with a gradient of buffer A [0.1% (v/v) formic acid in water] and buffer B [0.1% (v/v) formic acid in acetonitrile]. Separation was achieved using 2% buffer B for 0.6 min, followed by a linear gradient to 100% buffer B from 0.6 - 4.6 min, which was held at 100% buffer B from 4.6 - 5.6 min followed by a return to 2% buffer B from 5.6 - 6.6 min, along with 1 min post run. Spectra were recorded between a mass range of 50-1700 *m/z* at a rate of 10 spectra per second in positive polarity.

Supporting Information

Additional methods, *S. venezuelae* ATCC 10712 promoter and RBS platereader characterisation; Figure S1, optimisation of the MES buffer; Figure S2, Mg-glutamate and K-glutamate (mM) optimisation with A6-A9 cell-extract batches; Figure S3, characterisation of select promoters and RBS elements in *S. venezuelae* ATCC 10712; Figure S4, methylated DNA is not degraded in *S. venezuelae* ATCC 10712 cell-extracts during the active reaction period; Figure S5, *S. venezuelae* TX-TL activity of plasmid and PCR products under optimised conditions; Figure S6, SDS-PAGE of GUS synthesis in *S. venezuelae* TX-TL; Figure S7, SDS-PAGE of the melanin and haem operons in *S. venezuelae* TX-TL; Figure S8, mass spectrometry of the uroporphyrin III intermediate isolated from the semi-continuous reaction (from Figure 4); Table S1, plasmids created in this study; Table S2, PCR oligonucleotides; Table S3, annealing oligonucleotides; Table S4, sequencing primers; Table S5, promoter, RBS and RiboJ parts; List of DNA sequences.

Acknowledgments
The authors would like to thank Professor Jay Keasling (University of California) for providing the plasmid pAV-*gapdh*.

Funding
The author would like to acknowledge the following research support: EPSRC [EP/K038648/1] for SJM as a PDRA with PSF; Wellcome Trust sponsored ISSF fellowship for SJM with PSF at Imperial College London; Royal Society research grant [RGS\R1\191186] and Wellcome Trust SEED award [217528/Z/19/Z] for SJM at the University of Kent.

References

(1) Rutledge, P. J.; Challis, G. L. Discovery of Microbial Natural Products by Activation of Silent Biosynthetic Gene Clusters. *Nat. Rev. Microbiol.* **2015**, *13* (8), 509–523.

(2) Khatri, Y.; Hohlman, R. M.; Mendoza, J.; Li, S.; Lowell, A. N.; Asahara, H.; Sherman, D. H. Multicomponent Microscale Biosynthesis of Unnatural Cyanobacterial Indole Alkaloids. *ACS Synth. Biol.* **2020**, *9* (6), 1349–1360.

(3) Zhuang, L.; Huang, S.; Liu, W.-Q.; Karim, A. S.; Jewett, M. C.; Li, J. Total *in vitro* Biosynthesis of the Nonribosomal Macrolactone Peptide Valinomycin. *Metab. Eng.* **2020**, *60*, 37–44.

(4) Goering, A. W.; Li, J.; McClure, R. A.; Thomson, R. J.; Jewett, M. C.; Kelleher, N. L. *in vitro* Reconstruction of Nonribosomal Peptide Biosynthesis Directly from DNA Using Cell-Free Protein Synthesis. *ACS Synth. Biol.* **2017**, *6* (1), 39–44.

(5) Moore, S. J.; Lai, H.-E.; Needham, H.; Polizzi, K. M.; Freemont, P. S. *Streptomyces Venezuelae* TX-TL - a next Generation Cell-Free Synthetic Biology Tool. *Biotechnol. J.* **2017**, *12* (4), 1600678.

(6) Ozaki, T.; Yamashita, K.; Goto, Y.; Shimomura, M.; Hayashi, S.; Asamizu, S.; Sugai, Y.; Ikeda, H.; Suga, H.; Onaka, H. Dissection of Goadsporin Biosynthesis by *in vitro* Reconstitution Leading to Designer Analogues Expressed *in vivo*. *Nat. Commun.* **2017**, *8*, 14207.

(7) Li, J.; Wang, H.; Kwon, Y. C.; Jewett, M. C. Establishing a High Yielding *Streptomyces*-Based Cell-Free Protein Synthesis System. *Biotechnol. Bioeng.* **2017**, *114* (6), 1343–1353.

(8) Xu, H.; Liu, W.-Q.; Li, J. Translation Related Factors Improve the Productivity of a *Streptomyces*-Based Cell-Free Protein Synthesis System. *ACS Synth. Biol.* **2020**, *9* (5), 1221–1224.

(9) Siebels, I.; Nowak, S.; Heil, C. S.; Tufar, P.; Cortina, N. S.; Bode, H. B.; Grininger, M. Cell-Free Synthesis of Natural Compounds from Genomic DNA of Biosynthetic Gene Clusters. *ACS Synth. Biol.* **2020**, *9* (9), 2418–2426.

(10) Kuruma, Y.; Ueda, T. The PURE System for the Cell-Free Synthesis of Membrane Proteins. *Nat. Protoc.* **2015**, *10* (9), 1328–1344.

(11) Lavickova, B.; Maerkl, S. J. A Simple, Robust, and Low-Cost Method To Produce the PURE Cell-Free System. *ACS Synth. Biol.* **2019**, *8* (2), 455–462.

(12) Sun, Z. Z.; Hayes, C. A.; Shin, J.; Caschera, F.; Murray, R. M.; Noireaux, V. Protocols for Implementing an *Escherichia Coli* Based TX-TL Cell-Free Expression System for Synthetic Biology. *J. Vis. Exp.* **2013**, *50762* (79), e50762.

(13) Takahashi, M. K.; Chappell, J.; Hayes, C. A.; Sun, Z. Z.; Kim, J.; Singhal, V.; Spring, K. J.; Al-Khabouri, S.; Fall, C. P.; Noireaux, V.; Murray, R. M.; Lucks, J. B. Rapidly Characterizing the Fast Dynamics of RNA Genetic Circuitry with Cell-Free Transcription-Translation (TX-TL) Systems. *ACS Synth. Biol.* **2015**, *4* (5), 503–515.

(14) Gregorio, N. E.; Levine, M. Z.; Oza, J. P. A User's Guide to Cell-Free Protein Synthesis. *Methods Protoc* **2019**, *2* (1).

(15) Caschera, F.; Noireaux, V. Synthesis of 2.3 Mg/Ml of Protein with an All *Escherichia coli* Cell-Free Transcription-Translation System. *Biochimie* **2014**, *99* (1), 162–168.

(16) Jewett, M. C.; Swartz, J. R. Mimicking the *Escherichia coli* Cytoplasmic Environment Activates Long-Lived and Efficient Cell-Free Protein Synthesis. *Biotechnol. Bioeng.* **2004**, *86* (1), 19–26.

(17) Zawada, J. F.; Yin, G.; Steiner, A. R.; Yang, J.; Naresh, A.; Roy, S. M.; Gold, D. S.; Heinsohn, H. G.; Murray, C. J. Microscale to Manufacturing Scale-up of Cell-Free Cytokine Production-a New Approach for Shortening Protein Production Development Timelines. *Biotechnol. Bioeng.* **2011**, *108* (7), 1570–1578.
(18) Borkowski, O.; Koch, M.; Zettor, A.; Pandi, A.; Batista, A. C.; Soudier, P.; Faulon, J.-L. Large Scale Active-Learning-Guided Exploration for *in vitro* Protein Production Optimization. *Nat. Commun.* **2020**, *11* (1), 1872.
(19) Quast, R. B.; Kortt, O.; Henkel, J.; Dondapati, S. K.; Wüstenhagen, D. A.; Stech, M.; Kubick, S. Automated Production of Functional Membrane Proteins Using Eukaryotic Cell-Free Translation Systems. *J. Biotechnol.* **2015**, *203*, 45–53.
(20) Karim, A. S.; Heggestad, J. T.; Crowe, S. A.; Jewett, M. C. Controlling Cell-Free Metabolism through Physiochemical Perturbations. *Metab. Eng.* **2018**, *45*, 86–94.
(21) McManus, J. B.; Emanuel, P. A.; Murray, R. M.; Lux, M. W. A Method for Cost-Effective and Rapid Characterization of Engineered T7-Based Transcription Factors by Cell-Free Protein Synthesis Reveals Insights into the Regulation of T7 RNA Polymerase-Driven Expression. *Arch. Biochem. Biophys.* **2019**, *674*, 108045.
(22) Marshall, R.; Noireaux, V. Quantitative Modeling of Transcription and Translation of an All-*E. coli* Cell-Free System. *Sci. Rep.* **2019**, *9* (1), 11980.
(23) Moore, S. J.; MacDonald, J. T.; Wienecke, S.; Ishwarbhai, A.; Tsipa, A.; Aw, R.; Kylilis, N.; Bell, D. J.; McClymont, D. W.; Jensen, K.; Polizzi, K. M.; Biedendieck, R.; Freemont, P. S. Rapid Acquisition and Model-Based Analysis of Cell-Free Transcription-Translation Reactions from Nonmodel Bacteria. *Proc. Natl. Acad. Sci. U. S. A.* **2018**, *115* (19), E4340–E4349.
(24) Cheng, Q.; Xiang, L.; Izumikawa, M.; Meluzzi, D.; Moore, B. S. Enzymatic Total Synthesis of Enterocin Polyketides. *Nat. Chem. Biol.* **2007**, *3* (9), 557–558.
(25) Bai, C.; Zhang, Y.; Zhao, X.; Hu, Y.; Xiang, S.; Miao, J.; Lou, C.; Zhang, L. Exploiting a Precise Design of Universal Synthetic Modular Regulatory Elements to Unlock the Microbial Natural Products in *Streptomyces*. *Proc. Natl. Acad. Sci. U. S. A.* **2015**, *112* (39), 12181–12186.
(26) Phelan, R. M.; Sachs, D.; Petkiewicz, S. J.; Barajas, J. F.; Blake-Hedges, J. M.; Thompson, M. G.; Reider Apel, A.; Rasor, B. J.; Katz, L.; Keasling, J. D. Development of Next Generation Synthetic Biology Tools for Use in *Streptomyces venezuelae*. *ACS Synth. Biol.* **2017**, *6* (1), 159–166.
(27) Phelan, R. M.; Sekurova, O. N.; Keasling, J. D.; Zotchev, S. B. Engineering Terpene Biosynthesis in *Streptomyces* for Production of the Advanced Biofuel Precursor Bisabolene. *ACS Synth. Biol.* **2015**, *4* (4), 393–399.
(28) Han, A. R.; Park, J. W.; Lee, M. K.; Ban, Y. H.; Yoo, Y. J.; Kim, E. J.; Kim, E.; Kim, B. G.; Sohng, J. K.; Yoon, Y. J. Development of a *Streptomyces venezuelae*-Based Combinatorial Biosynthetic System for the Production of Glycosylated Derivatives of Doxorubicin and Its Biosynthetic Intermediates. *Appl. Environ. Microbiol.* **2011**, *77* (14), 4912–4923.
(29) Li, J.; Wang, H.; Jewett, M. C. Expanding the Palette of *Streptomyces*-Based Cell-Free Protein Synthesis Systems with Enhanced Yields. *Biochem. Eng. J.* **2018**, *130*, 29–33.
(30) Dopp, B. J. L.; Tamiev, D. D.; Reuel, N. F. Cell-Free Supplement Mixtures: Elucidating the History and Biochemical Utility of Additives Used to Support in Vitro Protein Synthesis in *E. coli* Extract. *Biotechnol. Adv.* **2019**, *37* (1), 246–258.

(31) Dudley, Q. M.; Nash, C. J.; Jewett, M. C. Cell-Free Biosynthesis of Limonene Using Enzyme-Enriched *Escherichia coli* Lysates. *Synth. Biol.* **2019**, *4* (1), ysz003.
(32) Wang, W.; Li, X.; Wang, J.; Xiang, S.; Feng, X.; Yang, K. An Engineered Strong Promoter for *Streptomycetes*. *Appl. Environ. Microbiol.* **2013**, *79* (14), 4484–4492.
(33) Yim, S. S.; Johns, N. I.; Park, J.; Gomes, A. L.; McBee, R. M.; Richardson, M.; Ronda, C.; Chen, S. P.; Garenne, D.; Noireaux, V.; Wang, H. H. Multiplex Transcriptional Characterizations across Diverse Bacterial Species Using Cell-Free Systems. *Mol. Syst. Biol.* **2019**, *15* (8), e8875.
(34) Jewett, M. C.; Calhoun, K. A.; Voloshin, A.; Wuu, J. J.; Swartz, J. R. An Integrated Cell-Free Metabolic Platform for Protein Production and Synthetic Biology. *Mol. Syst. Biol.* **2008**, *4* (220), 220.
(35) Earl, C. C.; Smith, M. T.; Lease, R. A.; Bundy, B. C. Polyvinylsulfonic Acid: A Low-Cost RNase Inhibitor for Enhanced RNA Preservation and Cell-Free Protein Translation. *Bioengineered* **2018**, *9* (1), 90–97.
(36) Myronovskyi, M.; Welle, E.; Fedorenko, V.; Luzhetskyy, A. β-Glucuronidase as a Sensitive and Versatile Reporter in Actinomycetes. *Appl. Environ. Microbiol.* **2011**, *77* (15), 5370–5383.
(37) Temme, K.; Zhao, D.; Voigt, C. A. Refactoring the Nitrogen Fixation Gene Cluster from *Klebsiella oxytoca*. *Proc. Natl. Acad. Sci. U. S. A.* **2012**, *109* (18), 7085–7090.
(38) Moore, S. J.; Lai, H.-E.; Kelwick, R. J. R.; Chee, S. M.; Bell, D. J.; Polizzi, K. M.; Freemont, P. S. EcoFlex: A Multifunctional MoClo Kit for *E. coli* Synthetic Biology. *ACS Synth. Biol.* **2016**, *5* (10), 1059–1069.
(39) Hecht, A.; Glasgow, J.; Jaschke, P. R.; Bawazer, L. A.; Munson, M. S.; Cochran, J. R.; Endy, D.; Salit, M. Measurements of Translation Initiation from All 64 Codons in *E. coli*. *Nucleic Acids Res.* **2017**, *45* (7), 3615–3626.
(40) Bibb, M. J.; Molle, V.; Buttner, M. J. Sigma(BldN), an Extracytoplasmic Function RNA Polymerase Sigma Factor Required for Aerial Mycelium Formation in *Streptomyces coelicolor* A3(2). *J. Bacteriol.* **2000**, *182* (16), 4606–4616.
(41) Chen, Y.-J.; Liu, P.; Nielsen, A. A. K.; Brophy, J. A. N.; Clancy, K.; Peterson, T.; Voigt, C. A. Characterization of 582 Natural and Synthetic Terminators and Quantification of Their Design Constraints. *Nat. Methods* **2013**, *10* (7), 659–664.
(42) Nielsen, A. A. K.; Der, B. S.; Shin, J.; Vaidyanathan, P.; Paralanov, V.; Strychalski, E. A.; Ross, D.; Densmore, D.; Voigt, C. A. Genetic Circuit Design Automation. *Science* **2016**, *352* (6281), aac7341.
(43) Garamella, J.; Marshall, R.; Rustad, M.; Noireaux, V. The All *E. coli* TX-TL Toolbox 2.0: A Platform for Cell-Free Synthetic Biology. *ACS Synth. Biol.* **2016**, *5* (4), 344–355.
(44) González-Cerón, G.; Miranda-Olivares, O. J.; Servín-González, L. Characterization of the Methyl-Specific Restriction System of *Streptomyces Coelicolor* A3(2) and of the Role Played by Laterally Acquired Nucleases. *FEMS Microbiol. Lett.* **2009**, *301* (1), 35–43.
(45) Bindels, D. S.; Haarbosch, L.; van Weeren, L.; Postma, M.; Wiese, K. E.; Mastop, M.; Aumonier, S.; Gotthard, G.; Royant, A.; Hink, M. A.; Gadella, T. W. J., Jr. mScarlet: A Bright Monomeric Red Fluorescent Protein for Cellular Imaging. *Nat. Methods* **2017**, *14* (1), 53–56.
(46) Matoba, Y.; Kihara, S.; Bando, N.; Yoshitsu, H.; Sakaguchi, M.; Kayama, K.; Yanagisawa, S.; Ogura, T.; Sugiyama, M. Catalytic Mechanism of the Tyrosinase

Reaction toward the Tyr98 Residue in the Caddie Protein. *PLoS Biol.* **2018**, *16* (12), e3000077.
(47) Heinemann, I. U.; Jahn, M.; Jahn, D. The Biochemistry of Heme Biosynthesis. *Arch. Biochem. Biophys.* **2008**, *474* (2), 238–251.
(48) Wildt, S.; Deuschle, U. CobA, a Red Fluorescent Transcriptional Reporter for *Escherichia coli*, Yeast, and Mammalian Cells. *Nat. Biotechnol.* **1999**, *17* (12), 1175–1178.

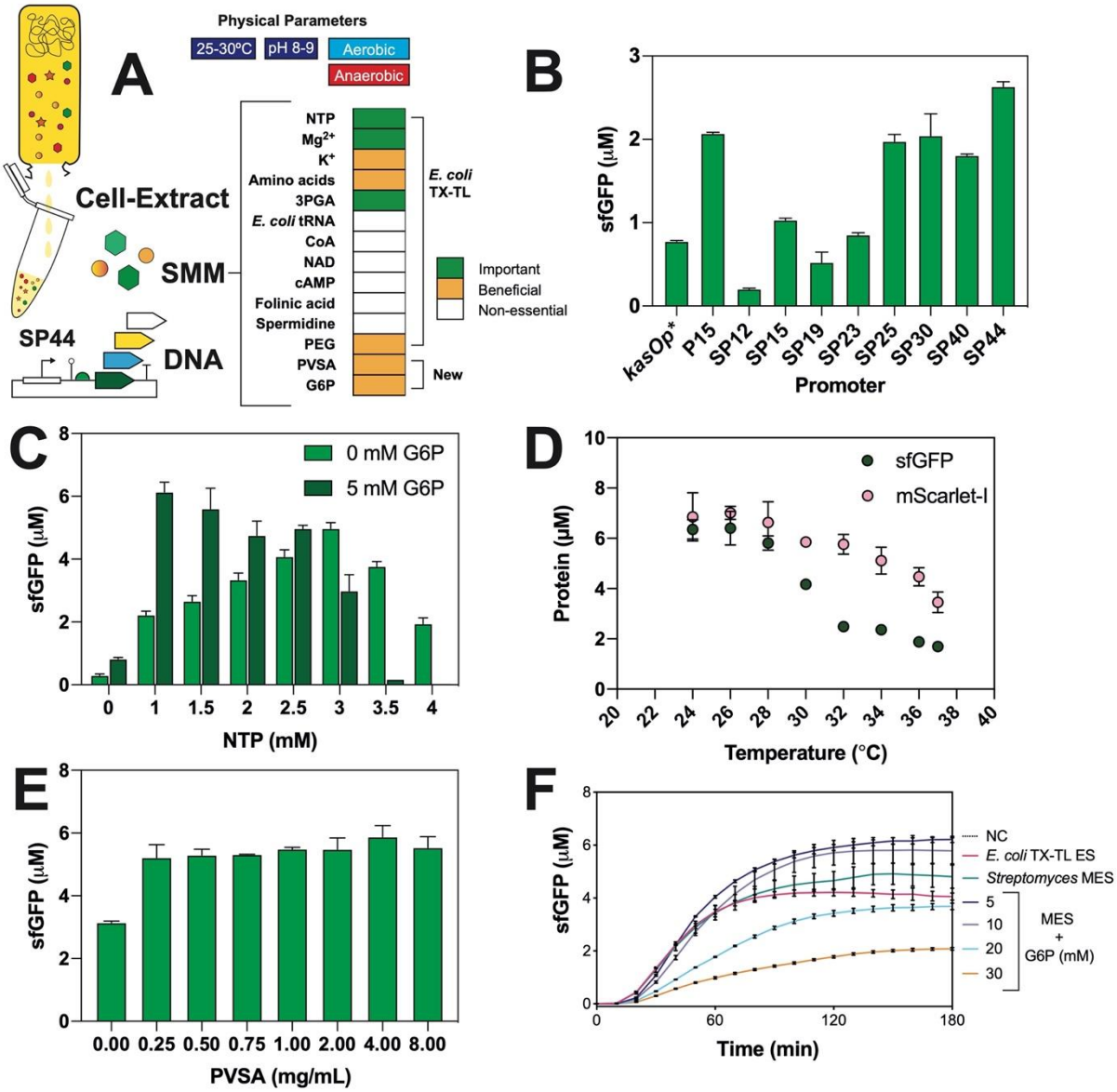

Figure 1. Overview of *Streptomyces* TX-TL optimisation. (A) Outline of physical and biochemical parameters of *Streptomyces* TX-TL and SMM buffer system. Optimisation of: (B) Promoter strength from Bai *et al* (19); (C) primary energy source; (D) Temperature; (E) PVSA; and (F) G6P. Error bars are representative of three technical measurements.

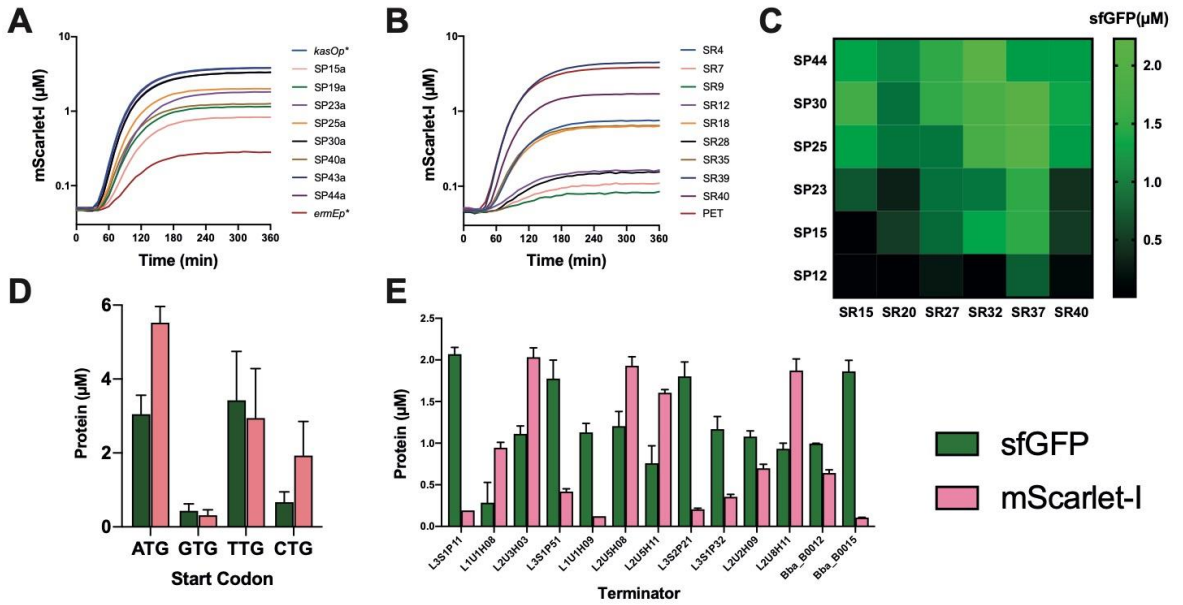

Figure 2. Part characterisation of *Streptomyces* regulatory elements: (A) Promoter-R15 capsid RBS-mScarlet-I; (B) *kasOp**-RBS-mScarlet-I; (C) Promoter-RBS-sfGFP combinations; (D) variable start codons (with sfGFP and mScarlet-I); and (E) variable Rho-independent terminators from Chen *et al* (34). For terminator plasmid design, see Moore *et al*[38]. 40 nM plasmid DNA was incubated in the optimised reaction conditions at 28°C as a technical triplicate repeat and repeated on two separate days. Unless otherwise stated, the SP44 promoter, PET RBS and Bba_B0015 were used in constructs, assembled into either pTU1-A (*E. coli*) or pSF-1 (*E. coli* and *Streptomyces* shuttle vector). Error bars are representative of three technical measurements.

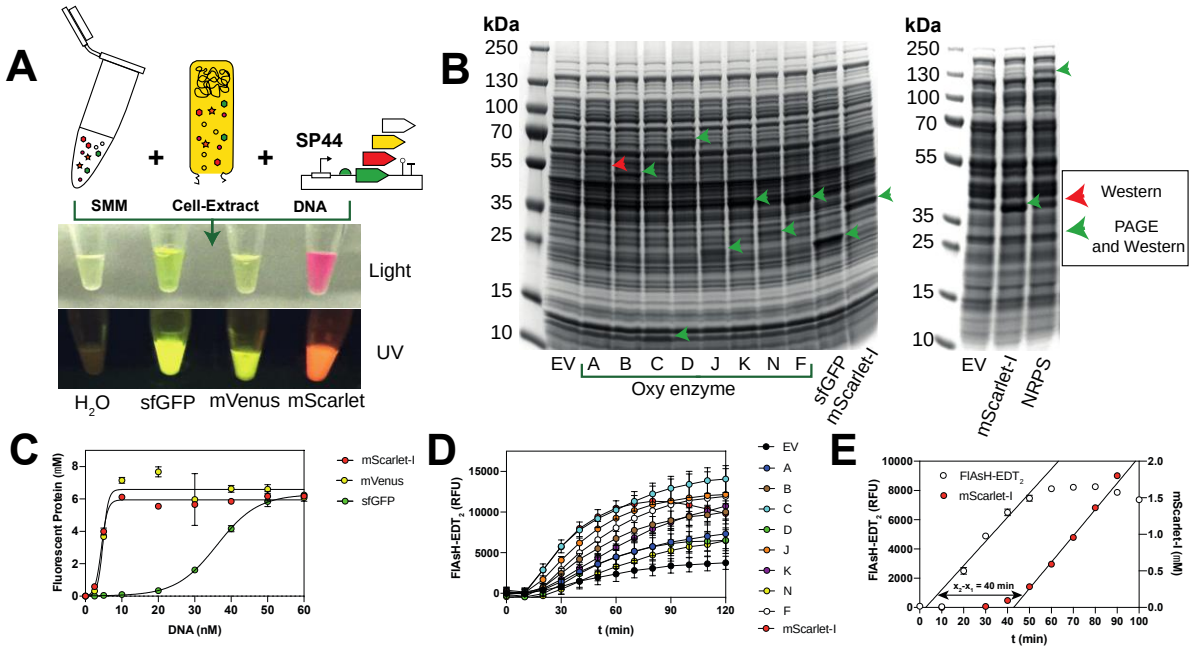

Figure 3. Robust and high-yield synthesis of high G+C (%) genes. (A) Synthesis of codon-optimised fluorescence proteins. (B) Denaturing PAGE of oxytetracycline biosynthetic proteins, fluorescence proteins and a representative NRPS (NH08_RS0107360 from *S. rimosus*). (C) Saturation of protein synthesis for sfGFP, mVenus and mScarlet-I with increasing DNA concentrations. (D) Real-time detection of protein synthesis with C-terminal FlAsH-EDT$_2$ tag system. (E) Estimation of mScarlet-I maturation time with real-time measurement of immature and mature protein synthesis. Error bars are representative of three technical measurements.

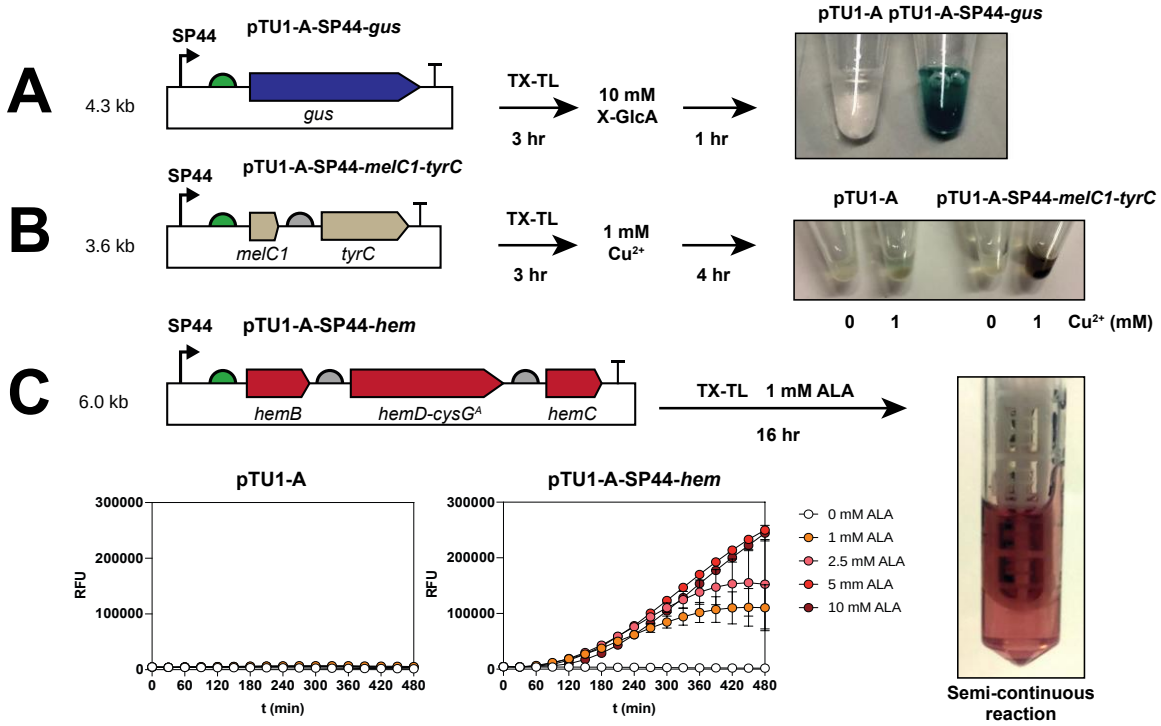

Figure 4. *Streptomyces* cell-free transcription, translation and biosynthesis. (A) Codon-optimised *E. coli* MG1655 GUS enzyme. (B) *S. venezuelae* DSM-40230 tyrosinase (TyrC) and copper metallochaperone (MelC1). (C) *S. venezuelae* DSM-40230 early-stage haem biosynthetic pathway, HemB, HemD-CysG^{A} and HemC. Addition of individual substrates and approximate timescales are indicated within the diagram. For details of batch and semi-continuous reaction conditions, please refer to methods. For a summary of the chemical intermediates, please see Figure S9. Melanin is a mixed family of pigments spontaneously produced from air oxidation of L-DOPA. Fluorescence error bars are representative of three technical measurements.